Binding of Hydroxamic Acid Inhibitors to Crystalline Thermolysin Suggests a Pentacoordinate Zinc Intermediate in Catalysis†

M. A. Holmes and B. W. Matthews*

ABSTRACT: The mode of binding of a series of hydroxamic acid derivatives, shown by Nishino and Powers [Nishino, N., & Powers, J. C. (1978) *Biochemistry 17*, 2846–2850] to be potent inhibitors of the zinc endopeptidase thermolysin, has been determined by X-ray crystallography. Carbobenzoxy-Gly-Gly-L-Leu-NHOH (K_i = 39 μM) was found to be slowly hydrolyzed in the crystals to yield L-Leu-NHOH, which is itself a good inhibitor (K_i = 190 μM). The structures of the complexes of L-Leu-NHOH and also HONH-benzylmalonyl-L-Ala-Gly-*p*-nitroanilide with crystalline thermolysin were determined at a resolution of 2.3 Å and refined to give crystallographic *R* values of 16.9% and 17.9%, respectively. L-Leu-NHOH binds "backward" in the active site with the hydroxamic acid moiety complexed with the zinc and the leucyl side chain occupying the hydrophobic specificity pocket at $R_{1'}$. The longer benzylmalonyl inhibitor binds in the "normal" mode, occupying sites $R_{1'}$, $R_{2'}$, and $R_{3'}$, with the hydroxamic group complexed with the zinc and the benzyl group in the specificity pocket. For both inhibitors, the hydroxamate group appears to bind in the anionic form, occupying very similar positions in each case. For both inhibitors, the hydroxamate moiety forms a novel bidentate complex with the zinc, with the carbonyl oxygen and the hydroxyl oxygen each approximately 2.0 Å from the metal ion. Thus, in both hydroxamate–thermolysin complexes, the zinc is pentacoordinate, with three ligands from the protein (His-142, His-146, and Glu-166) and two from the hydroxamate group. This is the first case in which a pentacoordinate complex has been observed for thermolysin, and the complex provides the first direct evidence supporting the idea that a pentacoordinate intermediate may participate in the mechanism of catalysis. It is particularly noteworthy that the *N*-hydroxyl group of the inhibitor forms a hydrogen bond to a carboxyl oxygen of Glu-143 and is close to the position which would be expected to be occupied by the water molecule which has been proposed previously to participate in general base catalysis.

During the past several years, it has become increasingly apparent that zinc metalloproteases occur widely and participate in a number of important biological and physiological processes. The role of carboxypeptidases A and B in digestion has long been recognized. Other metallopeptidases include collagenase, thought to be the destructive agent in arthritis (Harris & Krone, 1974), and the angiotensin-converting enzyme, which is important in regulating blood pressure (Peach, 1977). We have previously shown that the active site of thermolysin has striking similarities to that of carboxypeptidase A (Kester & Matthews, 1977a) even though the backbone conformations of the respective enzymes are otherwise very different. Also, known inhibitors of one of the zinc metalloproteases, when modified to take into account the differences in specificity of the respective enzymes, are often found to be equally good inhibitors of other members of the family [e.g., see Kam et al. (1979), Bolognesi & Matthews (1979), and Holmquist & Vallee (1979)]. Taken together, these observations suggest that all these zinc metalloproteases may have similarities in their active sites, and in their respective mechanisms of action (although not necessarily in their overall three-dimensional structures). For this reason, the crystallographic studies on thermolysin which we report here can be seen as part of a broad effort to understand the structure and function of a series of physiologically important enzymes.

Thermolysin is an extracellular, thermostable proteolytic enzyme of molecular weight 34 600 isolated from *Bacillus thermoproteolyticus* (Endo, 1962). The enzyme contains one catalytically essential zinc ion (Latt et al., 1969) and is a neutral endopeptidase specific for peptide bonds on the imino side of hydrophobic residues [e.g., see Matsubara et al. (1966)].

Crystallographic studies of the binding of inhibitors to thermolysin (Weaver et al., 1977; Kester & Matthews, 1977b; Bolognesi & Matthews, 1979) have provided evidence for the mode of binding of extended substrates to the enzyme and have suggested a mechanism of action for peptide hydrolysis.

In this paper, we describe the mode of binding to crystalline thermolysin of hydroxamate inhibitors. These compounds were introduced by Nishino & Powers (1978) and were shown to be potent inhibitors of thermolysin, with inhibition constants as low as 10^{-6} M. The three inhibitors studied crystallographically are carbobenzoxy-Gly-Gly-L-Leu-NHOH (hereafter ZGGL-NHOH)[1] (K_i = 39 μM), HONH-benzylmalonyl-L-Ala-Gly-*p*-nitroanilide (HONH-BzmAGNA; K_i = 0.43 μM), and L-Leu-NHOH (K_i = 190 μM).

It is shown that these inhibitors bind to the enzyme with the hydroxamate group complexed to the zinc in a novel 5-coordinate arrangement. This is the first instance in which a 5-coordinate zinc complex of thermolysin has been observed and provides evidence supporting the idea that a 5-coordinate complex involving the carbonyl oxygen of the substrate and a water molecule may be an intermediate in catalysis.

Materials and Methods

Thermolysin, 3 times recrystallized, was obtained from Calbiochem. The inhibitors ZGGL-NHOH, HONH-

† From the Institute of Molecular Biology and Departments of Chemistry and Physics, University of Oregon, Eugene, Oregon 97403. *Received May 20, 1981.* This research was supported in part by grants from the National Science Foundation (PCM-8014311), the National Institutes of Health (GM20066, GM28138, and 5T32-GM07759), and the M. J. Murdock Charitable Trust.

[1] Abbreviations used: Z, *N*-carbobenzoxy [$C_6H_5CH_2OC(O)$–]; Bzm, benzylmalonyl [$-COCH(CH_2C_6H_5)CO-$]; HONH-BzmAGNA, HONH-benzylmalonyl-L-alanylglycine-*p*-nitroanilide; ZGGL-NHOH, carbobenzoxyglycylglycyl-L-leucyl-NHOH; Tris–acetate, 2-amino-2-(hydroxymethyl)-1,3-propanediol acetate; FAGLA, furylacryloylglycyl-leucinamide.

0006-2960/81/0420-6912$01.25/0

Table I: Intensity Statistics for Inhibitor Data Sets

	L-Leu-NHOH	HONH-BzmAGNA
no. of film packs	18	18
no. of reflections	12029	11989
resolution (Å)	2.3	2.3
av R_{sym}[a] (%)	6.3	6.5
R_{merge}[b] (%)	2.6	2.1
av isomorphous difference (%)	8.2	13.4

[a] $R_{sym} = \Sigma|I - \bar{I}|/\Sigma I$ for symmetry-related intensities recorded on the same film. [b] $R_{merge} = \Sigma|F - \bar{F}|/\Sigma F$ for reflections measured on different films.

BzmAGNA (available only as a racemic mixture), and L-Leu-NHOH were a gift of Dr. J. C. Powers (Nishino & Powers, 1978).

Native crystals of thermolysin were obtained as described previously (Colman et al., 1972) and were stored in a mother liquor of 0.01 M calcium acetate, 0.01 M Tris–acetate, and 5% (v/v) dimethyl sulfoxide, pH 7.2. Crystals of thermolysin–inhibitor complexes were obtained by soaking native crystals in mother liquor in which the inhibitor had been dissolved. The concentrations of inhibitor and the soaking times were as follows: ZGGL-NHOH, 1.0 mM for at least 3 days; HONH-BzmAGNA, 0.1 mM for at least 2 days; L-Leu-NHOH, 1.0 mM for 15 days.

X-ray diffraction data for the thermolysin–inhibitor complexes were collected by using the method of precession photography. The X-ray source was an Elliot GX-6 rotating anode generator, and crystals were exposed for 48 h. A summary of the data collection statistics for the two inhibitors for which three-dimensional data were collected is given in Table I.

The usual difference electron density maps with coefficients $F_{complex} - F_{nat}$ were calculated but were not suitable for model building since the native enzyme has many water molecules bound in the active site which are displaced by bound inhibitors (Kester & Matthews, 1977b). Instead, maps with coefficients $2F_{complex} - F_{nat}$ were calculated for the two inhibitors, and Kendrew–Watson models were fitted to the maps by using an optical comparator (Richards, 1968; Colman et al., 1972). Atomic coordinates were obtained by placing markers on the map sections in the corresponding density, guided by the wire model. Values of x and y were measured directly from the sections, and z values were estimated to within half a section (0.37 Å).

The native thermolysin structure was refined at 2.3-Å resolution to a crystallographic residual of 0.182 by using a restrained least-squares refinement program written by Dr. W. Hendrickson (Hendrickson & Konnert, 1980). Additional details will be given elsewhere. Structure factor amplitudes and phases were calculated from this refined native structure with any water molecules in the active site within 2 Å of each inhibitor removed. These calculated native structure factors (F_{nat}^{calcd}) were used to obtain additional difference maps of the form ($F_{complex} - F_{nat}^{calcd}$) for the two inhibitors. The coordinates of the inhibited complexes were refined by using the Hendrickson program. The idealized stereochemistry used in the refinement for the hydroxamic acid groups was that of the anion. The refined native thermolysin and water molecule coordinates together with the raw inhibitor model coordinates were used as starting coordinate sets for the respective inhibitor refinements. Refinement was halted when the improvement in the complex coordinates had levelled off. During the refinement of the complexes, several arginine side chains of the protein moved large distances away from their correct positions. This physically unreasonable behavior appeared to be due to some quirk in the refinement program which we could not locate. Therefore, the refinement was completed by using a restrained least-squares refinement program written by Dr. L. Ten Eyck. Table II summarizes the results of refinement of the complexes.

Table II: Refinement Statistics for Inhibitor Complexes

	L-Leu-NHOH	HONH-BzmAGNA
initial R value[a]	0.195	0.234
final R value	0.169	0.179
rms deviation from ideality		
bond length (Å)	0.045	0.047
bond angle (deg)	5.9	6.1
planarity (trigonal) (Å)	0.007	0.007
planarity (other planes) (Å)	0.012	0.012
no. of refinement cycles	12	8
no. of reflections used (10.0–2.3 Å)	11854	11797
no. of atoms	2597	2606
no. of bonds	2500	2514
no. of bond angles	3395	3410
no. of trigonal planes	66	66
no. of other planes	375	378
no. of variables	10389	10425

[a] R value = $\Sigma|F_{obsd} - F_{calcd}|/\Sigma|F_{obsd}|$.

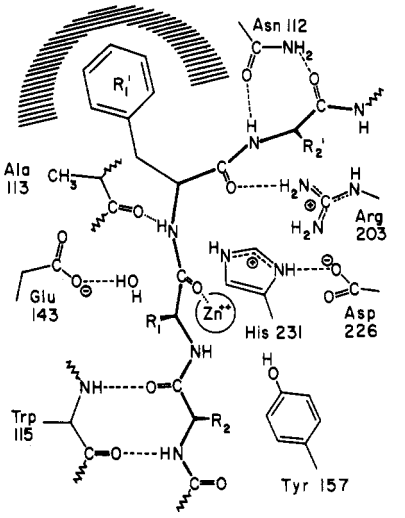

FIGURE 1: Schematic drawing showing the geometry of binding of extended substrates to thermolysin inferred from the observed binding of a variety of inhibitors. The interactions for R_2 are inferred from model building.

Results

Binding of ZGGL-NHOH. ZGGL-NHOH was expected to bind with its C terminus, which contains the hydroxamic acid group, at the zinc ion of the thermolysin active site and with the remainder of the molecule oriented as a typical peptide substrate would be (Figure 1). A difference map with coefficients $F_{complex} - F_{nat}$ had density in the active-site region (Figure 2A), providing clear evidence that the inhibitor was bound to the crystalline enzyme. However, on inspection of the $2F_{complex} - F_{nat}$ difference map, it was seen that there was inhibitor density close to the active-site zinc ion, but not at the R_1, R_2, or R_3 binding sites. [The nomenclature used for the individual amino acid residues R_2, R_1, $R_{1'}$, $R_{2'}$, etc. and the active site subsites S_1, $S_{1'}$, etc. follows that of Schechter & Berger (1967) and is also shown in Figure 1.] Instead, there was density in the hydrophobic pocket which gives thermolysin its primary specificity (the $R_{1'}$ binding site) and very weak

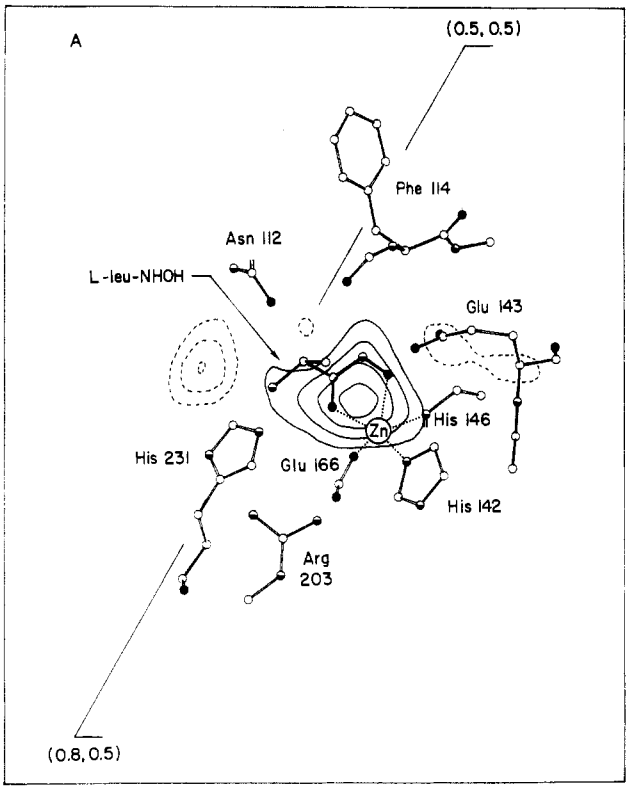

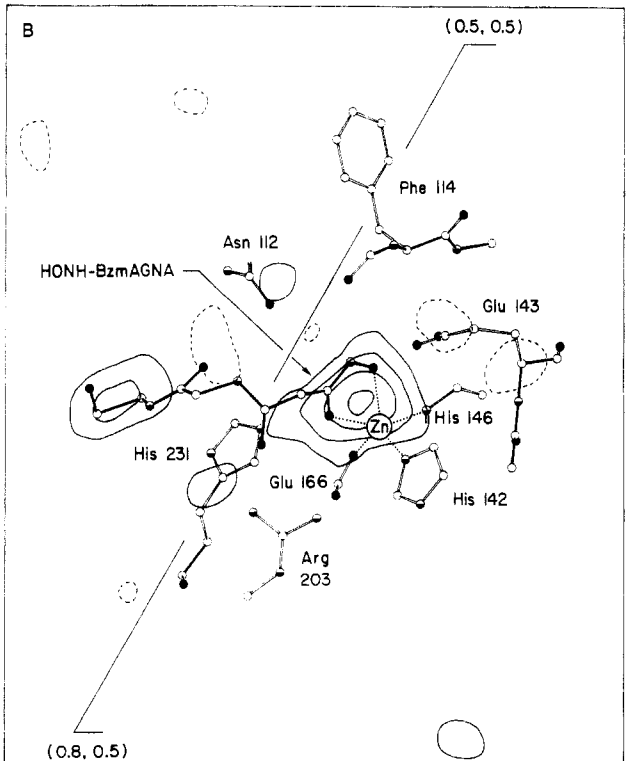

FIGURE 2: Portion of the difference electron density maps for the bound hydroxamate inhibitors calculated with coefficients of the form $F_{complex} - F_{nat}$ and isomorphous-replacement phases. The section shown, $z = -0.045$, passes close to the zinc ion and includes the highest feature in the difference map. Solid contours indicate positive density, and broken contours indicate negative density. Contours are drawn at an arbitrary equal level. The interpretation of the strong density feature as the bound hydroxamate moiety is shown, as are protein atoms within 3 Å of this section. Carbon atoms are drawn open, oxygen atoms solid, and nitrogen atoms half-solid. (A) L-Leu-NHOH–inhibitor complex; (B) HONH-BzmAGNA–inhibitor complex.

density at the $R_{2'}$ binding site. In other words, it appeared that the inhibitor was binding backward in the active-site cleft. We concluded that the inhibitor had been hydrolyzed by the enzyme and that the products, presumably L-Leu-NHOH and, to a lesser extent, Gly-L-Leu-NHOH, remained bound, while the remainder of the inhibitor had diffused away. Subsequently, Nishino & Powers (1978) confirmed this result by using thin-layer chromatography and found a half-life of about 2 days for the hydrolysis of ZGGL-NHOH by thermolysin. As an additional check, we diffused L-Leu-NHOH into native thermolysin crystals and calculated a difference projection map between thermolysin–ZGGL-NHOH and thermolysin–L-Leu-NHOH which we found to be essentially featureless, confirming that the actual inhibitor bound to thermolysin was, for the most part, L-Leu-NHOH.

Initially a Kendrew model of Gly-L-Leu-NHOH was fitted to the difference map, with the glycyl residue occupying the weak density at the $R_{2'}$ binding site, and the leucyl residue at the $R_{1'}$ binding site, with its hydrophobic side chain in the pocket. The hydroxamic acid group was seen to be interacting with the zinc ion and also forming a hydrogen bond to the carbonyl oxygen of Ala-113. The exact nature of the interaction with the zinc was not clear although it did appear that the hydroxamic acid might be acting as a bidentate zinc ligand.

Calculation of an $F_{complex} - F_{nat}^{calcd}$ difference map (Figure 3A) resulted in electron density corresponding to the inhibitor which was very similar to that seen previously except in one respect. Instead of the continuous weak density which had been modeled with the glycyl residue of Gly-L-Leu-NHOH, the new map contained two separate weak peaks. One of the peaks was at exactly the position of one of the water molecules that had been removed from the coordinate list to calculate the native structure amplitudes. The other peak appeared to be a water molecule hydrogen bonded to the amino group of the leucyl residue of the inhibitor.

In metal chelates, the hydroxamic acid group is in the anionic, rather than the protonated, form (Nielands, 1966; Zalkin et al., 1966). The anion exists in two resonance forms (Bauer & Exner, 1974):

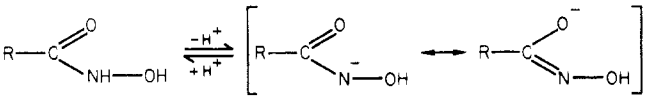

A model of L-Leu-NOH$^-$, based on bond lengths and angles observed in small molecules (Bowen et al., 1958; Andrews et al., 1965), differs from the model of the protonated form mainly in that the two oxygen atoms of the hydroxamic acid group are closer together in the anion. The anionic form of the inhibitor gave a much improved fit to the electron density map, leading to the conclusion that it is the anion of L-Leu-NHOH which binds to thermolysin.

In the $2F_{complex} - F_{nat}^{calcd}$ difference map, it could be seen that the nitrogen of the hydroxamic acid group was not hydrogen bonded to the carbonyl oxygen of Ala-113, as had been thought might be the case. The absence of this hydrogen bond is also consistent with the anionic form of L-Leu-NHOH binding to the enzyme.

Binding of HONH-BzmAGNA. The shape of the electron density around the thermolysin active-site zinc in the $F_{complex} - F_{nat}$ and $2F_{complex} - F_{nat}$ maps calculated for HONH-BzmAGNA was very similar to that in the corresponding map for ZGGL-NHOH (Figure 2A, B). Again, it was obvious that the hydroxamic acid group was interacting with the zinc, probably as a bidentate ligand, but in exactly what manner was not clear. As before, the nitrogen of the hydroxamic acid

Table III: Refined Inhibitor Coordinates[a]

	X	Y	Z	B
		L-Leu-NHOH		
N	52.91	16.55	−4.35	29
CA	52.00	17.68	−4.75	29
C	52.57	18.76	−5.67	30
O	53.63	18.70	−6.37	29
N2	51.84	19.83	−5.65	29
N2O	52.48	20.73	−6.49	28
CB	52.03	18.47	−3.35	27
CG	52.92	17.72	−2.37	27
CD1	54.28	17.67	−3.14	26
CD2	53.03	18.25	−0.95	24
H_2O	50.04	21.24	−8.04	21
H_2O	50.36	17.86	−7.88	31
		HONH-BzmAGNA		
OH1	52.31	20.21	−6.04	21
N1	52.09	19.38	−4.87	23
C1	53.12	18.53	−4.89	24
O1	54.03	18.60	−5.93	23
C2	53.78	16.28	−3.67	25
O2	55.04	16.16	−3.61	27
CA2	53.26	17.58	−3.76	24
CB2	52.73	18.00	−2.60	24
CG2	53.45	18.12	−1.27	23
CD12	52.71	17.71	−0.21	22
CD22	54.70	18.63	−1.13	22
CE12	53.26	17.80	1.00	23
CE22	55.25	18.70	0.07	22
CZ2	54.53	18.28	1.15	23
N3	52.76	15.31	−3.67	27
C3	53.04	13.25	−4.99	29
O3	52.25	14.07	−5.61	30
CA3	53.26	13.79	−3.59	28
CB3	52.90	13.11	−2.48	28
N4	53.64	12.11	−5.50	31
C4	53.90	10.22	−6.79	32
O4	53.02	9.96	−5.80	34
CA4	53.36	11.81	−6.87	32
H_2O	50.04	21.24	−8.04	21
H_2O	50.36	17.86	−7.88	31

[a] The coordinates are in angstroms relative to a right-handed coordinate system, with the origin at the crystallographic origin and X parallel to a^*, Y parallel to b, and Z parallel to c.

group appeared to be hydrogen bonded to the carbonyl oxygen of Ala-113. The phenyl ring of the benzylmalonyl group was in the hydrophobic pocket with the second carbonyl oxygen hydrogen bonded to the side chain of Arg-203. When the wire model of the inhibitor was built, the D stereoisomer was used, as it gave a better fit to the map. The $R_{2'}$ residue of the inhibitor, i.e., alanine, formed two main-chain hydrogen bonds with the side chain of Asn-112. Residue $R_{3'}$, glycine, had no interactions with the enzyme, and the nitroaniline group appeared to assume so many different conformations that there was no density for it in the map.

Examination of $F_{complex} - F_{nat}^{calcd}$ and $2F_{complex} - F_{nat}^{calcd}$ maps for HONH-BzmAGNa yielded the same conclusions as had been reached for the inhibitor L-Leu-NHOH, namely, that the hydroxamic acid group was in its anionic form and that there was no hydrogen bond between the nitrogen of the hydroxamic acid group and Ala-113 (Figure 3B).

Refinement of the Inhibited Complexes. The model coordinates for the inhibitors in the two thermolysin–inhibitor complexes were stereochemically idealized and refined to crystallographic R values of 16.9% and 17.9%, respectively (Table II). Table III gives the two sets of refined inhibitor coordinates, and the complete lists of refined coordinates for the protein–inhibitor complexes have been deposited at the Protein Data Bank (Bernstein et al., 1977). The estimated

Table IV: Thermolysin–Inhibitor Distances

protein	L-Leu-NHOH	distance (Å)
Asn-112 OD1	N	3.3
Ala-113 O	N2[a]	3.5
Glu-143 OE1	OH2[a]	2.7
His-231 NE2	O[a]	3.0
protein	HONH-BzmAGNA	distance (Å)
Asn-112 OD1	N3	3.0
Asn-112 ND2	O3	3.8
Ala-113 O	N1[a]	3.3
Glu-143 OE1	OH1[a]	2.7
Arg-203 NEE1	O2	2.5
His-231 NE2	O1[a]	2.9

[a] Atoms in the respective hydroxamate groups.

Table V: Zinc–Ligand Distances (Å)

ligand	L-Leu-NHOH	HONH-BzmAGNA
His-142 NE2	2.3	2.2
His-146 NE2	2.0	2.0
Glu-166 OE1	2.0	2.1
inhibitor carbonyl O	2.0	2.1
inhibitor hydroxyl O	2.1	2.3

accuracy of the inhibitor coordinates is about 0.2 Å. Table IV gives selected distances between protein atoms and inhibitor atoms in the two refined complexes, and Figure 4 shows the structures of the complexes in the vicinity of the active site.

In each complex, the distance between the carbonyl oxygen of Ala-113 and the nearby inhibitor nitrogen atom (3.5 and 3.3 Å) is too large for a hydrogen bond to occur (a good hydrogen-bonding distance is 2.8 Å; a distance of 3.0 Å would correspond to a weak hydrogen bond). There is a hydrogen bond between the hydroxyl oxygen of each inhibitor and OE1 of Glu-143 which was not apparent in the difference maps. A weak hydrogen bond exists between OD1 of Asn-112 and a backbone nitrogen of HONH-BzmAGNA, but the other possible hydrogen bond between Asn-112 and the inhibitor does not appear to be made. As seen previously in other inhibitors, a backbone carbonyl oxygen of HONH-BzmAGNA is hydrogen bonded to the guanidinium group of Arg-203. The hydroxamate group of the inhibitors binds to the active-site zinc atom in a bidentate manner (Table V).

For each of the hydroxamate inhibitors, there is no indication that binding occurs to any of the four calcium ions bound to the thermolysin molecule. There is also no indication that the inhibitors remove any of the metal ions.

Discussion

Comparison of Kinetic and Crystallographic Results. Kinetic data on the inhibition of thermolysin by various peptide–hydroxamic acid derivatives are given in Table VI (Nishino & Powers, 1978, 1979). The abilities of these compounds to inhibit the enzyme can be compared in order to ascertain which elements of the compounds contribute to binding, and the inferences from the kinetic data agree well with those obtained from the crystallographic analyses of the two inhibitors ZGGL-NHOH and HONH-BzmAGNA.

For compounds related to ZGGL-NHOH, it can be seen that modification of the hydroxamic acid group either at the hydroxyl oxygen or at the nitrogen, or replacement of the hydroxamic acid group with an amino group, results in a significant loss of inhibitory ability. This suggests that the hydroxamic acid group is an essential element in this series

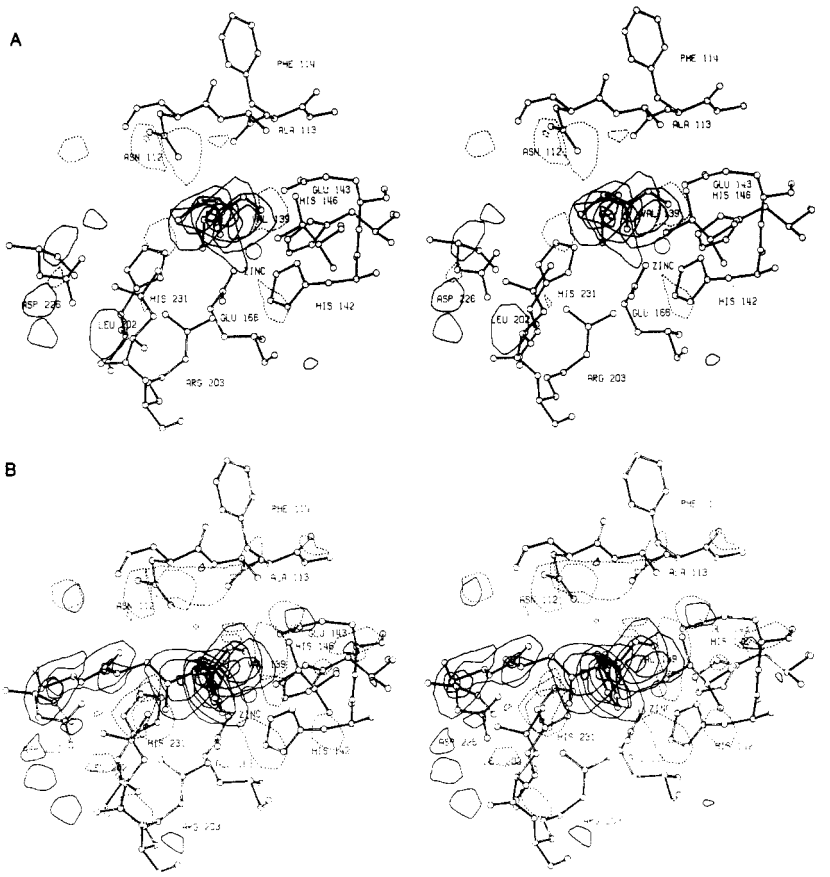

FIGURE 3: Stereo drawings showing the refined inhibitor complexes superimposed on a difference electron density map with coefficients of the form $F_{complex} - F_{nat}^{calcd}$ (see text). (A) L-Leu-NHOH–inhibitor complex; (B) HONH-BzmAGNA–inhibitor complex.

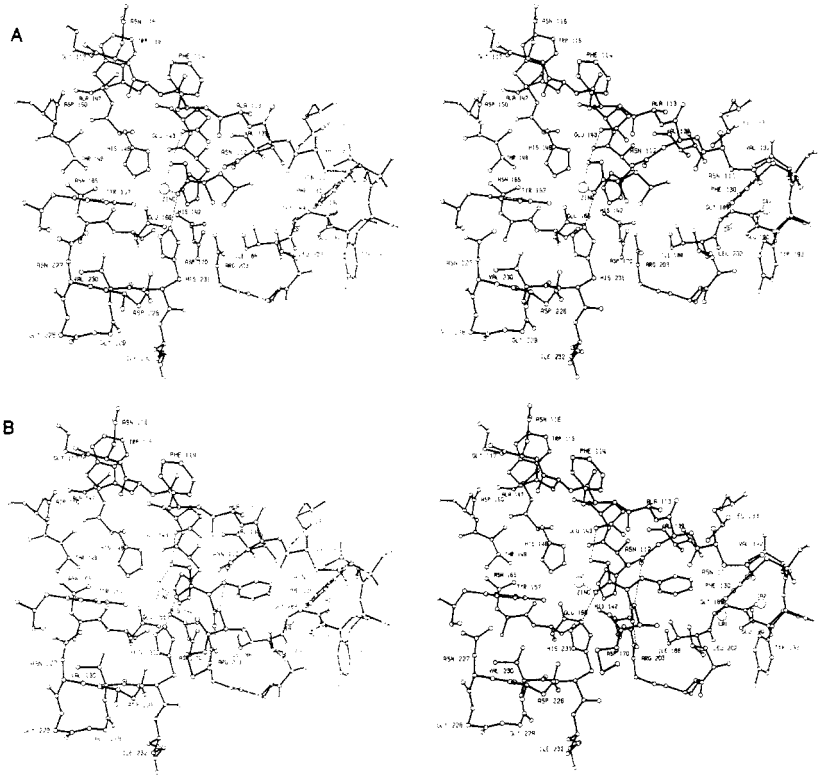

FIGURE 4: Stereoviews of the hydroxamate inhibitors bound to the extended thermolysin active site. The direction of view is from the left of that shown in Figure 3. (A) Thermolysin–L-Leu-NHOH complex; (B) thermolysin–HONH-BzmAGNA complex.

of inhibitors. Similarly, comparison of the K_i's of ZGG-NHOH and ZGL-NHOH shows that the presence of a hydrophobic side chain is important for binding. An examination of the K_i's of ZGL-NHOH and ZGGL-NHOH and their optical antipodes suggests that the inhibitors may bind initially with a normal peptide orientation, since, with a reverse orientation, the D optical isomers would be expected to be as good or better inhibitors. It should be noted that hydrolysis of the

Table VI: Kinetic Data for Inhibitors[a]

	K_i (μM)
L-Leu-NHOH	190
Z-Gly-L-Leu-NH_2	no inhibition[b]
Z-Gly-L-Leu-NHOH	13
Z-Gly-D-Leu-NHOH	59
Z-Gly-L-Leu-N(CH_3)OH	2230
Z-Gly-L-Leu-$NHOCH_3$	no inhibition
Z-Gly–Gly-NHOH	940
Z-Gly-Gly-L-Leu-NHOH	39
Z-Gly-Gly-D-Leu-NHOH	250
HONH-Bzm-OEt	20[c]
HONH-Bzm-L-Ala-Gly-NA	0.43[c,d]
HONH-Bzm-L-Ala-Gly-NH_2	0.66[c]
HONH-Mal-L-Ala-Gly-NH_2	1100
OH-Bzm-L-Ala-Gly-NH_2	420[c]

[a] Taken from Nishino & Powers (1978, 1979). [b] K_m value = 21 000 μM. [c] The benzylmalonyl residue is racemic. [d] I_{50} value at 1 mM substrate concentration.

L-Leu-NHOH derivatives by the enzyme is sufficiently slow that it does not affect the results of the kinetic experiments (Nishino & Powers, 1978).

Inspection of Figure 4A shows why methylation of the hydroxamate nitrogen decreases the affinity of the inhibitor by a factor of 170 (Table VI). As discussed previously, this nitrogen is 3.5 Å from the carbonyl oxygen of Ala-113 so that methylation results in steric interference between the bound inhibitor and the enzyme. Methylation of the hydroxyl oxygen of the hydroxamate moiety no doubt prevents binding because the methyl group would sterically interfere with Glu-143 (Figure 4A).

When compounds related to HONH-BzmAGNA are considered, a comparison of the K_i values of HO-BzmAG-NH_2 and HONH-BzmAG-NH_2 indicates that the hydroxamic acid group again makes a major contribution to the binding. Replacement of the benzylmalonyl group with an unsubstituted malonyl moiety results in a substantial loss of inhibitory activity, suggesting that the presence of a hydrophobic side chain adjacent to the hydroxamic acid is important for binding. The existence of enzyme–inhibitor interactions beyond the $R_{1'}$ residue is indicated by the decrease in K_i upon addition of a dipeptide to the compound HONH-Bzm-OEt. All these conclusions are consistent with the mode of binding of HONH-BzmAGNA to thermolysin which has been deduced from the crystallographic data (Figure 4B).

Our results confirm the main conclusions reached by Nishino & Powers (1978, 1979). In particular, the data given here provide the first definitive evidence that hydroxamate inhibitors of thermolysin bind with the hydroxamic acid moiety complexed with the zinc. Also the crystallographic data show that the mode of hydroxamate binding is not monodentate (Nishino & Powers, 1978), but bidentate (Nishino & Powers, 1979), with the *N*-hydroxycarboxamido group in the cis configuration. It is reasonable to infer that the geometry of hydroxamate binding to other zinc proteases is very similar to that observed for thermolysin.

Hydrolysis of ZGGL-NHOH. Our results show clearly that ZGGL-NHOH is slowly hydrolyzed by crystalline thermolysin. As discussed above, ZGGL-NHOH appears to bind predominantly in a backward mode in the active-site cleft, with the hydroxamate moiety complexed with the zinc. However, the inhibitor must sometimes bind in a mode which permits hydrolysis of the Gly-Leu bond, i.e., with the glycine at R_1 and the leucine at $R_{1'}$ with its side chain in the specificity pocket. Eventually, all of the ZGGL-NHOH is hydrolyzed, leaving the product L-Leu-NHOH, a poorer but still good inhibitor of thermolysin (K_i = 190 μM), to occupy the active site, as is observed in the crystallographic study.

Value of Refinement. In common with other laboratories, we found the crystallographic refinement of the native thermolysin structure and the thermolysin–inhibitor complexes to be particularly helpful in two ways. First, once the native thermolysin structure had been refined, reliable calculated native structure factors, with the contribution of water molecules in the enzyme's active site removed, were available. This made it possible to calculate difference electron density maps which were not confused by the displacement of water molecules. In the case of the inhibitor ZGGL-NHOH, the difference map indicated that the molecules actually binding to thermolysin consisted entirely of L-Leu-NHOH, rather than a mixture of L-Leu-NHOH and Gly-L-Leu-NHOH, as had been indicated by the initial map calculated with the isomorphous replacement phases.

Also, in the $2F_{complex} - F_{nat}^{calcd}$ difference maps, there was no density indicating an interaction between the carbonyl oxygen of Ala-113 and the hydroxamic acid group. The apparent absence of this hydrogen bond helped confirm the idea that it is the hydroxamate form of the inhibitors which binds to thermolysin.

The second benefit of the refinement process was that it provided reliable atomic coordinates from which interatomic distances could be calculated. From these distances, it was quite clear which protein atoms were interacting with which inhibitor atoms. In the process of refinement, some pairs of atoms which had been thought to interact moved apart, while some unsuspected interactions became apparent. For example, a tentative hydrogen bond between a carbonyl oxygen atom of HONH-BzmAGNA and the side-chain nitrogen atom of Asn-112 is not supported by the refined coordinates (Table IV). Also, the lack of a hydrogen bond between the hydroxamate nitrogen and Ala-113 is confirmed in the refined complex structures (Table IV). On the other hand, the interaction between the hydroxamate hydroxyl oxygen and the Glu-143 side chain which is seen in both refined structures was not apparent until refinement took place.

Mechanism of Catalysis. A catalytic mechanism for thermolysin has been proposed by Kester & Matthews (1977b) [see also Pangburn & Walsh (1975)]. In the first step, the substrate is bound to the enzyme in the manner shown in Figure 1. In the next step, Glu-143 promotes the nucleophilic attack of a water molecule on the carbonyl carbon of the scissile peptide bond, which has been somewhat polarized by the zinc ion. Concurrently, His-231 donates a proton to the nitrogen of the scissile bond. This intermediate is tetrahedral at both the carbon and nitrogen atoms and is stabilized by hydrogen bonds with Glu-143 and His-231 and an electrostatic interaction with the zinc ion. In the final step, the carbon–nitrogen bond of the intermediate breaks to yield the two product peptides. The burial of the charged groups Glu-143 and Zn^{2+} in a nonpolar environment upon binding of substrate to the enzyme may be one of the driving forces of catalysis. It is presumed that the favorable interactions between enzyme and substrate discussed above provide the free energy required to bury the charged groups. Once buried, Glu-143 is a strong base capable of mediating the attack of a water molecule upon the carbonyl carbon, and the zinc ion acts as a Lewis acid to polarize the carbonyl bond. The subsequent neutralization of Glu-143 and Zn^{2+} provides the free energy needed to form the tetrahedral transition state.

When the catalytic mechanism is considered in more detail, the enzyme–substrate complex could be formed in two ways.

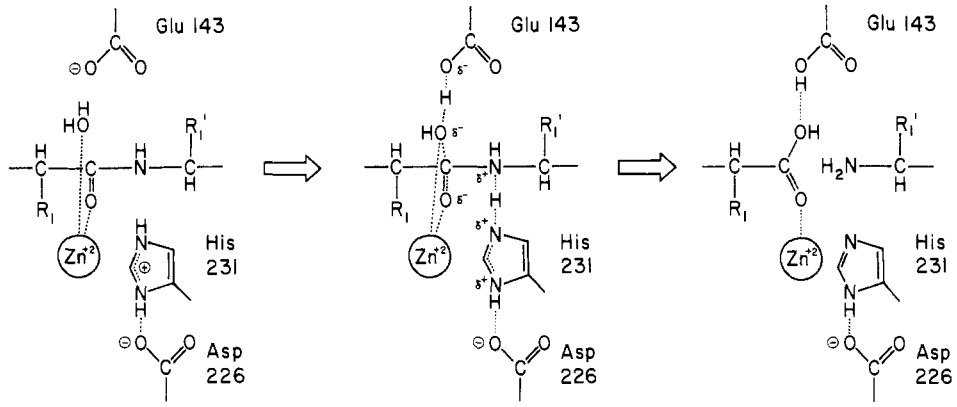

FIGURE 5: Schematic illustration of the proposed mechanism of catalysis for thermolysin.

In the first mechanism, the water molecule would be displaced from the zinc ion, leaving an empty ligand site, which the substrate carbonyl oxygen would then fill. The second and more likely mechanism has the zinc ion becoming temporarily 5-coordinate by interacting with both the water molecule and the incoming substrate. Model binding of this intermediate shows that this change in coordination geometry would cause the water molecule to move in a direct line toward Glu-143. The appealing aspect of this second mechanism is that it avoids postulating the existence of an empty ligand site at the zinc ion. Also, the displaced water molecule is translocated to the vicinity of Glu-143 much more efficiently than in the first mechanism.

This 5-coordinate zinc mechanism, illustrated in Figure 5, combines elements of a general base-catalyzed reaction with a direct catalytic role for zinc as suggested by studies of model compounds [e.g., see Buckingham et al. (1974), Woolley (1975), Fife & Squillacote (1977, 1978), Wells & Bruice (1977), and Groves & Dias (1979)]. In the case of thermolysin, the native enzyme has a water molecule, or possibly a hydroxide ion, coordinated tetrahedrally to the zinc. As the substrate enters the active-site cleft, and begins to form a favorable complex with the enzyme, the zinc-bound water molecule is translocated toward Glu-143, and, at the same time, the carbonyl oxygen of the scissile peptide bond begins to coordinate with the metal. As the water molecule approaches Glu-143, the negative charge enhances its nucleophilicity. Thus, the zinc ion not only polarizes the substrate carbonyl bond but also helps determine the correct alignment of the carbonyl bond and the attacking nucleophile.

The 5-coordinate zinc mechanism for the binding of substrate to thermolysin is supported by experiments in which the active-site zinc ion has been replaced by other metal ions. Zinc and cobalt give the highest enzyme activities toward the chromophoric substrate FAGLA, 100% and 200%, respectively, while Mn^{2+}-substituted thermolysin has 10% activity (Holmquist & Vallee, 1974; Bigbee & Dahlquist, 1974). The substitution of Cu^{2+}, Cd^{2+}, or Hg^{2+} into the thermolysin active site results in inactive forms of the enzyme (Holmquist & Vallee, 1974). Of these metals, zinc and cobalt are the ones most often observed with trigonal bipyramidal coordination (Cotton & Wilkinson, 1972). Zinc and cobalt are also able to change their coordination state relatively easily, compared to other metals (Lindskog, 1970; Vallee & Williams, 1968; Prince & Woolley, 1972). Furthermore, the enzymatic activity of the various metal-substituted thermolysins does *not* correlate with the "hardness" of the metals as Lewis acids. Zn^{2+}, Co^{2+}, and Cu^{2+} are all classified as intermediate Lewis acids (Pearson, 1966), yet the respective metal-substituted thermolysins have activities ranging from maximum to zero. Mn^{2+} is a hard Lewis acid but yields an active enzyme. Also there is no correlation between enzymatic activity and the size of the metal ion (Cu^{2+} and Zn^{2+}, for example, are practically identical in size). Clearly, the role of the metal is more than that of a simple Lewis acid.

The possibility of a pentacoordinate intermediate has been suggested for other enzymes which have a catalytically essential zinc. Woolley (1975) suggested on the basis of studies of model catalysts for carbonic anhydrase that a zinc-bound water molecule could ionize to provide an effective nucleophile in the form of a metal-bound hydroxide. Following their crystallographic studies of the structure of carbonic anhydrase, Kannan et al. (1977) incorporated zinc hydroxide in a mechanism in which the carbon dioxide substrate bound weakly at a fifth zinc coordination site. Also Dworschack & Plapp (1977) and Boiwe & Brändén (1977) have proposed that a pentacoordinate transition state complex with both a hydroxyl ion and a neutral alcohol bound to the zinc may occur in alcohol dehydrogenase. On the basis of structural comparisons of the zinc environments of carbonic anhydrase, alcohol dehydrogenase, carboxypeptidase A, and thermolysin, Rossmann & Argos (1978) have postulated that a 5-coordinate intermediate might occur for each of these zinc-containing enzymes.

In the case of thermolysin, there has been no direct evidence to date for anything other than 4-fold coordination at the active-site zinc. Now, for the first time, the hydroxamate inhibitors provide a clear example of 5-fold coordination. In both hydroxamate complexes, the zinc is 5-coordinate, the ligands being three protein side chains which contribute two nitrogens and one oxygen, and the two oxygens of the hydroxamic acid group of the inhibitor. The respective ligand distances, all of which are close to 2.0 Å, are given in Table V. The coordination is distorted trigonal bipyramidal, with Glu-166 and the hydroxyl oxygen of the inhibitor as the axial ligands and His-142, His-146, and the carbonyl oxygen of the inhibitor as the equatorial ligands (see Figure 6). This structure resembles quite closely the proposed 5-coordinate zinc reaction intermediate, in which the two axial zinc ligands are Glu-166 and the catalytically important water molecule, and one of the other three ligands is the carbonyl oxygen of the substrate. In particular, it is striking to see for both inhibitors that the hydroxamate hydroxyl oxygen forms a strong hydrogen bond (distance 2.7 Å) to the carboxyl oxygen OE1 of Glu-143, just as the water molecule would be expected to do.

In order to show the 5-coordinate geometry relative to the position occupied by a peptide substrate of thermolysin, in Figure 7 we have superimposed the hydroxamate group, as observed for L-Leu-NHOH, on the inhibitor β-phenyl-

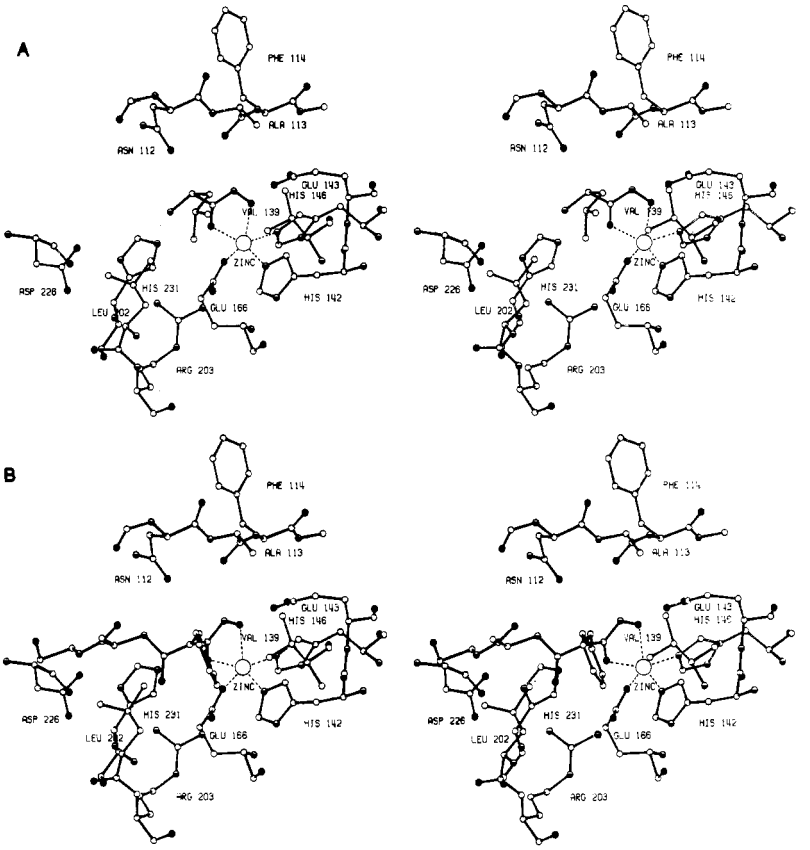

FIGURE 6: Stereoviews showing the similar 5-fold zinc coordination observed in the two hydroxamate–thermolysin complexes. (A) L-Leu-NHOH complex; (B) HONH-BzmAGNA complex.

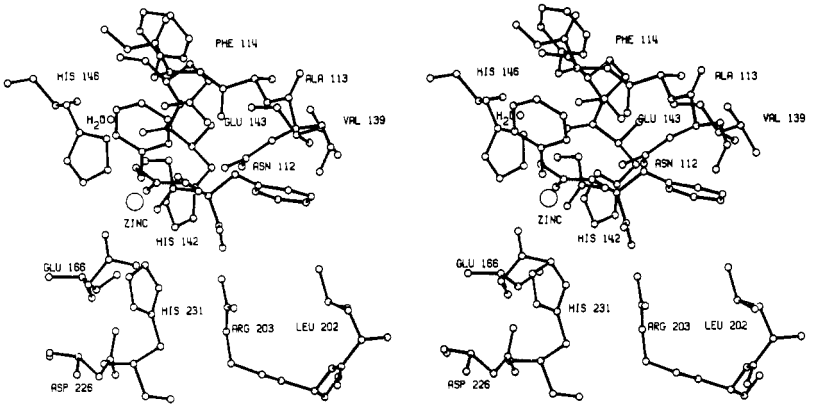

FIGURE 7: Stereo drawing of the hydroxamate group of L-Leu-NHOH (open bonds) superimposed on the inhibitor β-phenylpropionyl-L-phenylalanine (solid bonds) in the thermolysin active site.

propionylphenylalanine (Kester & Matthews, 1977b). As can be seen, the hydroxyl oxygen of the inhibitor is located within the triangle formed by the carbonyl carbon of the "substrate", the zinc ion, and oxygen OE1 of Glu-143. During catalysis, the attacking water molecule would be expected to occupy a very similar position. Of course, the position occupied by the hydroxyl oxygen is constrained by the geometry of the inhibitor and need not coincide exactly with that of the water molecule.

Certainly, the best evidence for the existence of the 5-coordinate zinc intermediate during catalysis would be the direct observation of such an intermediate formed with a true substrate. One way this might be achieved is with the technique of low-temperature crystallography, in which substrate is diffused into the protein crystal at subzero temperatures (the temperature being chosen to give a half-life for the enzyme–substrate complex of at least several days, thus making it possible to collect diffraction data). We have attempted such a study, but have not been successful to date. Crystals of thermolysin can readily be equilibrated with cryosolvents such as, for example, 80% (v/v) ethanol–water or methanol–water and give diffraction patterns at room temperature which are quite similar to those of the native enzyme. However, when these crystals are cooled, they crack at about 0 °C, which is not a sufficiently low temperature to obtain stable enzyme–substrate complexes.

It is interesting to note that the two inhibitors we have studied, one with the hydroxamate group at its C terminus and the other with the hydroxamate at the N terminus, both bind with the hydroxamate moiety complexed to the zinc in a very similar manner, but the peptide portions of the respective inhibitors run in opposite directions. We choose the inhibitor ZGGL-NHOH for crystallographic analysis with the hope that the study would, in part, reveal the mode of binding of an extended thermolysin substrate in the subsites to the "left"

of the zinc, in particular, subsites R_2, R_3, etc. However, no new information of these subsites is provided, and we have to rely on model building to infer the presumed interactions between protein and substrate (i.e., for residue R_2 in Figure 1). In remains unclear whether a suitably designed C-terminal peptide hydroxamate might bind in the "normal" mode in subsites S_1, S_2, etc. One obvious requirement for such an inhibitor is that the residue adjacent to the hydroxamate should not be one, such as leucine, which binds readily in the $R_{1'}$ specificity pocket. Replacing the leucine, as used here, with another residue would, hopefully, prevent the enzymatic hydrolysis of the inhibitor and would also reduce the tendency of this side chain to occupy the $R_{1'}$ subsite, as happens for both inhibitors described here.

Acknowledgments

In writing this paper, we have benefited from the unpublished laboratory notes of Dr. William Kester, in particular his comments concerning a possible 5-coordinate zinc intermediate in the mechanism of thermolysin. We are grateful to Dr. James Powers for generous gifts of hydroxamic acid inhibitors and for continued helpful discussions. Also we thank Dr. F. W. Dahlquist for helpful discussions concerning the mechanism of thermolysin and Drs. L. F. Ten Eyck, M. F. Schmid, and L. H. Weaver for help with implementing the refinement programs.

References

Andrews, A. L., Bishop, R. J., Cleaver, B., Dennard, A. E., Henn, D. E., Loader, B. E., Mackay, A. L., Mendel, H., Morgan, D. J., Owston, P. G., & Phillips, D. C. (1965) in *Tables of Interatomic Distances and Configuration in Molecules and Ions, Supplement* (Mitchell, A. D., Somerfield, A. E., & Cross, L. C., Eds.) The Chemical Society, London.

Bauer, L., & Exner, O. (1974) *Angew. Chem., Int. Ed. Engl. 13*, 376–384.

Bernstein, F. C., Koetzle, T. F., Williams, G. J. B., Jr., Meyer, E. F., Brice, M. D., Rodgers, J. R., Kennard, O., Shimanouchi, T., & Tasumi, M. (1977) *J. Mol. Biol. 112*, 535–542.

Bigbee, W. L., & Dahlquist, F. W. (1974) *Biochemistry 13*, 3542–3549.

Boiwe, T., & Brändèn, C. I. (1977) *Eur. J. Biochem. 77*, 173–179.

Bolognesi, M. C., & Matthews, B. W. (1979) *J. Biol. Chem. 254*, 634–639.

Bowen, H. J. M., Donohue, J., Jenkin, D. G., Kennard, O., Wheatley, P. J., & Whiffen, D. H. (1958) in *Tables of Interatomic Distances and Configuration in Molecules and Ions* (Mitchell, A. D., & Cross, L. C., Eds.) The Chemical Society, London.

Buckingham, D. A., Keene, F. R., & Sargeson, A. M. (1974) *J. Am. Chem. Soc. 96*, 4981–4983.

Colman, P. M., Jansonius, J. N., & Matthews, B. W. (1972) *J. Mol. Biol. 70*, 701–724.

Cotton, F. A., & Wilkinson, G. (1972) *Advanced Inorganic Chemistry*, pp 503ff, 845ff, 875ff, 903ff, Interscience, New York.

Dworschack, R. T., & Plapp, B. V. (1977) *Biochemistry 16*, 111–116.

Endo, S. (1962) *J. Ferment. Technol. 40*, 346–353.

Fife, T. H., & Squillacote, V. L. (1977) *J. Am. Chem. Soc. 99*, 3762–3769.

Fife, T. H., & Squillacote, V. L. (1978) *J. Am. Chem. Soc. 100*, 4787–4793.

Groves, J. T., & Dias, R. M. (1979) *J. Am. Chem. Soc. 101*, 1033–1035.

Harris, E. D., & Krone, S. M. (1974) *N. Engl. J. Med. 291*, 557, 605, 652.

Hendrickson, W. A., & Konnert, J. H. (1980) in *Computing in Crystallography* (Diamond, R., Ramaseshan, S., & Venkatesan, K., Eds.) pp 13.01–13.23, Indian Academy of Sciences, Bangalore.

Holmquist, B., & Vallee, B. L. (1974) *J. Biol. Chem. 249*, 4601–4607.

Holmquist, B., & Vallee, B. L. (1979) *Proc. Natl. Acad. Sci. U.S.A. 76*, 6216–6220.

Kam, C.-M., Nishino, N., & Powers, J. C. (1979) *Biochemistry 18*, 3032–3038.

Kannan, K. K., Petef, M., Fridborg, K., Cid-Dresdner, H., & Lougren, S. (1977) *FEBS Lett. 73*, 115–119.

Kester, W. R., & Matthews, B. W. (1977a) *J. Biol. Chem. 252*, 7704–7710.

Kester, W. R., & Matthews, B. W. (1977b) *Biochemistry 16*, 2506–2516.

Latt, S. A., Holmquist, B., & Vallee, B. L. (1969) *Biochem. Biophys. Res. Commun. 37*, 333–339.

Lindskog, S. (1970) *Struct. Bonding (Berlin) 8*, 154–196.

Matsubara, H., Sasaki, R., Singer, A., & Jukes, T. H. (1966) *Arch. Biochem. Biophys. 115*, 324–331.

Nielands, J. B. (1966) *Struct. Bonding (Berlin) 1*, 59–108.

Nishino, N., & Powers, J. C. (1978) *Biochemistry 17*, 2846–2850.

Nishino, N., & Powers, J. C. (1979) *Biochemistry 18*, 4340–4347.

Pangburn, M. K., & Walsh, K. A. (1975) *Biochemistry 14*, 4050–4054.

Peach, M. J. (1977) *Physiol. Rev. 57*, 313–370.

Pearson, R. G. (1966) *Science (Washington, D.C.) 151*, 172–177.

Prince, R. H., & Woolley, P. R. (1972) *Angew. Chem., Int. Ed. Engl. 11*, 408–417.

Richards, F. M. (1968) *J. Mol. Biol. 37*, 225–230.

Rossman, M. G., & Argos, P. (1978) *Mol. Cell. Biochem. 21*, 161–182.

Schechter, I., & Berger, A. (1967) *Biochem. Biophys. Res. Commun. 27*, 157–162.

Vallee, B. L., & Williams, R. J. P. (1968) *Proc. Natl. Acad. Sci. U.S.A. 59*, 498–505.

Weaver, L. H., Kester, W. R., & Matthews, B. W. (1977) *J. Mol. Biol. 114*, 119–132.

Wells, M. A., & Bruice, T. C. (1977) *J. Am. Chem. Soc. 99*, 5341–5356.

Woolley, P. (1975) *Nature (London) 258*, 677–682.

Zalkin, A., Forrester, J. D., & Templeton, D. H. (1966) *J. Am. Chem. Soc. 88*, 1810–1814.